Climate Dynamics (2023) 60:1225–1238
https://doi.org/10.1007/s00382-022-06344-8

Mechanism of the summer rainfall variation in Transitional Climate Zone in East Asia from the perspective of moisture supply during 1979–2010 based on the Lagrangian method

Qiulin Wang[1,2] · Gang Huang[1,2,5,8] · Lin Wang[3] · Jinling Piao[4] · Tianjiao Ma[4] · Peng Hu[4] · Chakrit Chotamonsak[6] · Atsamon Limsakul[7]

Received: 11 November 2021 / Accepted: 7 May 2022 / Published online: 27 June 2022

Abstract

Transitional Climate Zone (TCZ) over East Asia, characterized by semi-arid climate, is ecologically fragile environment with limited water resources, making atmospheric moisture supply being the key influential factor. This study investigates the moisture sources of summer (JJA) rainfall in the TCZ over East Asia and associated impact during 1979–2010 with the Lagrangian particle dispersion model. Seven moisture source regions and associated contribution are quantified: Eurasia continent to northwest of the TCZ (EC, 32.14%), central-eastern China (CEC, 16.62%), western Pacific Ocean (WPO, 8.58%), South China Sea and Indonesia (SCSI, 2.99%), Bay of Bengal (BOB, 1.4%), Arabian Sea (AS, 0.71%) and local evaporation (TCZ, 32.58%). The direct moisture contribution from ocean (13.67%) is much less than those from the continent (81.34%), due to the great loss en-route. In particular, the local evaporation not only contributes the most moisture among 7 selected source regions, but also exerts the greatest influence in summer precipitation variability in TCZ. Furthermore, the moisture related to summer rainfall over TCZ conveyed by westerlies and monsoon are discriminated according to the dominant system of moisture source regions. It is found that moisture contributions from summer monsoon system (30.3%) and the mid-latitude westerlies (32.14%) dominant areas are quite close. However, further analysis shows that summer monsoon system takes more responsibility for inter-annual fluctuation of summer precipitation in TCZ from the perspective of moisture supply, followed by local evaporation and mid-latitude westerlies.

Keywords Moisture sources · Summer precipitation · Transitional Climate Zone · Lagrangian method

✉ Gang Huang
hg@mail.iap.ac.cn

✉ Lin Wang
linwang@mail.iap.ac.cn; wang_lin@mail.iap.ac.cn

[1] State Key Laboratory of Numerical Modeling for Atmospheric Sciences and Geophysical Fluid Dynamics, Institute of Atmospheric Physics, Chinese Academy of Sciences, Beijing 100029, China

[2] College of Earth and Planetary Sciences, University of Chinese Academy of Sciences, 100049 Beijing, China

[3] CAS Key Laboratory of Regional Climate-Environment for Temperate East Asia, Institute of Atmospheric Physics, Chinese Academy of Sciences, Beijing, China

[4] Center for Monsoon System Research, Institute of Atmospheric Physics, Chinese Academy of Sciences, 100190 Beijing, China

[5] Laboratory for Regional Oceanography and Numerical Modeling, Qingdao National Laboratory for Marine Science and Technology, 266237 Qingdao, China

[6] Department of Geography, Faculties of Social Sciences, Chiang Mai University, Chiang Mai, Thailand

[7] Environmental Research and Training Center, Klong 5, Klong Luang, Technopolis, Pathumthani 12120, Thailand

[8] Institute of Atmospheric Physics, Chinese Academy of Sciences, Beijing 100029, China

1 Introduction

The Transitional Climate Zone (TCZ) over East Asia, also known as the monsoon transitional zone between monsoon and non-monsoon regions, stretches from the eastern fringe of the Tibetan Plateau to Northeast China. Due to the influence of the interannual variability of the monsoon and the mid-latitude westerly winds, this area is featured by large gradients of climate and biome (Ou and Qian 2006; Chen et al. 2018, 2019). It is also the farming-pastoral ecotone (FPE) in China, whose response of vegetation growth to climate change, especially to precipitation variation, is relatively sensitive (Ou and Qian 2006; Lu and Jia 2013). In addition, TCZ is featured by semi-arid climate and highly vulnerable to climate change. With the pace of global warming, extreme weather events will become more probable in China (Wang and Chen 2014). In particular, the TCZ has experienced the largest warming over East Asia and the most significant aridification over the past century (Li et al. 2015; Huang et al. 2017, 2019). A new global desertification vulnerability index constructed by Huang et al. (2020) in which both climate change and human activity are considered, suggested that this area have a high risk of desertification. There have been studies about the dry-wet conditions of TCZ. Wang et al. (2017) suggested the precipitation variation is the main fact affecting inter-annual fluctuation of both fringes of TCZ while increasing evaporation plays an important role in the long-term trend. Our previous study also investigated the temporal and spatial variation of TCZ in summer during 1961–2018, finding that the dry and wet conditions of the transition zone vary greatly from year to year, which are mainly caused by summer precipitation (Wang et al. 2021). Therefore, it is necessary to explore the mechanism of precipitation change in TCZ.

Sufficient water vapor supply is one of the necessary conditions for precipitation formation. Characterized by semi-arid climate, limited water supply makes it necessary to explore moisture source of TCZ. Eulerian method is a common method to analyze water vapor transportation and the budget of water vapor in an atmospheric column with grid data (Trenberth and Guillemot 1995; Simmonds et al. 1999; Oshima et al. 2015; Zhu et al. 2020). However, it provides simple moisture transport paths and fails to show detailed information on the geographical sources of the moisture since the meteorological field is transient (Sodemann et al. 2008). On the contrary, lagrangian analog can make up these defects by facilitating better source-sink relationship since it allows researchers to trace along the air block trajectory and shows changes of spatial position and moisture content (Zhihong et al. 2013; Salih et al. 2015; Peng et al. 2020; Wang et al. 2020).

Lagrangian particle dispersion models (LPDMs) are proved versatile tools for simulating the transport and turbulent mixing of gases and aerosols in the atmosphere, and have been widely used in hydrologic cycle research, such as the Hybrid Single-Particle Lagrangian Integrated Trajectory (HYSPLIT) model (Hao et al. 2014; Stein et al. 2015; Wang et al. 2020) and the FLEXible PARTicle (FLEXPART) model (Pisso et al. 2019). FLEXPART model has been widely used in addressing moisture transport. Nieto et al. (2006) examined the main sources over the Sahel, suggesting recycling was the dominant moisture source over the Sahel. Salih et al. (2015) identified source regions of water vapor for Sahelian Sudan during the monsoon period with FLEXPART. In their latter study(Salih et al. 2016), they compared it with results comes from atmospheric general circulation model with an embedded moisture-tracing module (Community Atmosphere Model version 3), finding that two approaches differ when comparing individual regions, but are in better agreement when neighboring regions of similar atmospheric flow features are grouped together. They suggested that longer back trajectories would have been necessary to capture a more realistic transport, although it also implies larger errors. FLEXPART has been also used for the study of the moisture origin of precipitation over Asia (Sun and Wang 2013, 2015; Huang and Cui 2015; Peng et al. 2020) explored moisture sources of central Asia which is associated with the deep low trough over central Asia and the anticyclone over North Africa and western Asia in the lower and middle troposphere. Moisture sources of the Tibetan Plateau during the wet season have also been investigated by Chen et al. (2019). Sun and Wang (2015) studied the major atmospheric moisture sources affecting three sub-regions of East China, which is conducted for non-precipitation and precipitation cases of summertime and wintertime. Bin et al. (2013) also revealed major moisture sources contributed to summer water vapor of the lower Yangtze River Basin with different transport timescales.

Large efforts from the scientific community have been devoted toward a better understanding climate change during summer in East Asia, especially the adjustment of summer monsoon system and middle and high latitude systems (Qian et al. 2010; Huang et al. 2011, 2012; Wang et al. 2017; Chen et al. 2019; He and Zhou 2020). As an interaction region of warm and wet air mass controlled by summer monsoon systems and dry and cold air mass by the mid-latitude westerlies (Huang et al. 2017; Wang et al. 2017), there also have been studies devoted into variations of the wet-dry conditions of TCZ and its driving mechanisms. Wang et al. (2021) suggests the interannual variation of summer wet-dry condition in TCZ is mainly influenced by EASM circulation and the low-pressure anomaly over Mongolian area. Model sensitive experiments conducted by Zhao et al. (2019) and Piao et al. (2017) showed that SST anomalies in the tropical

central-eastern Pacific and the NTA are both key drivers for inter-annual and decadal variations of precipitation over the MTZ in China during summer. The teleconnection pattern over Eurasia excited by warming sea surface temperature in the North Atlantic is concerned with the interdecadal change of summer rainfall in TCZ in the 1990s (Piao et al. 2017; Zhao et al. 2020). However, it is difficult to quantify the effect of different systems on the wet-dry conditions of TCZ. Lagrange diagnose provide a new thinking. Here, we applied the latest version of FLEXPART (FLEXPART_10.4v) to trace back the trajectories of the air mass over TCZ during summer (JJA) from 1979 to 2010, and to identify main source regions and quantify their contributions to the summer rainfall of TCZ.

This paper is organized as follows. The next section describes the model, datasets, methods to simulate Lagrangian precipitation and identify moisture source regions and moisture contribution quantification. Section 3 demonstrates model results including the simulated precipitation, main moisture transport paths and identification of major moisture source regions, along with quantification of moisture contributions from main source regions and how they behave in wet/dry year. The roles of monsoon system and mid-high latitude systems in inter-annual variation of summer precipitation in TCZ will also be discussed in this section. Finally, we conclude and summarize our findings in Sect. 4.

2 Data and method

2.1 Data

The FLEXPART model is driven by the National Centers for Environmental Prediction–Climate Forecast System Reanalysis (NCEP–CFSR) 6-hourly forecast data (Saha et al. 2010) from 1979 to 2010, including land cover, temperature, relative humidity, and three-dimensional winds at 42 levels with a horizontal resolution of 0.5° × 0.5°. In fact, CFSR 6-hourly forecast data has been updated regularly until present. However, data product from March 2011 onwards is created based on the second version of the NCEP Climate Forecast System (CFSv2), which only operates 11 years. Thereby, to avoid the possible discontinuity before and after 2011, we confine our study period from 1979 to 2010. Such more-than-30 years is long enough to perform the moisture source detection.

Furthermore, the model simulation quality of summer precipitation in TCZ is verified by both observation and reanalysis datasets. The observation daily precipitation from 1979 to 2010 is retrieved from the National Meteorological Information Center, with a spatial resolution of 0.5° × 0.5°(Xu et al. 2019). On the other hand, monthly reanalyzed precipitation used in this study is obtained from the Japanese 55-year Reanalysis (JRA-55), a global reanalysis product constructed by the Japan Meteorological Agency (Kobayashi et al. 2015; Harada et al. 2016), with a horizontal resolution of 1.25° × 1.25°. And 6-hourly reanalysis datasets from JRA-55 are also employed to analyze the moisture transport flux field during summer in east Asia including horizontal wind, specific humidity, and surface pressure.

2.2 Model simulation and target region

TCZ is the junction of arid and humid regions, with large spatial gradient of precipitation. In our previous study, TCZ boundary was delimited by summer Arid Index (SM_AI), which is defined as total summer precipitation (MJJAS) divided by total summer potential evaporation during 1979–2010 (Wang et al. 2021). Due to the complexity of TCZ boundary, a simplified parallelogram is used here as the boundary of the target region (Fig. 1). Since the summer rainy season in TCZ begins in early June and ends in late August (Wang et al. 2021), we explored the moisture sources of precipitation in TCZ from June to August during 1979–2010. According to the Eulerian water vapor budget equation (Trenberth and Guillemot 1995), E-P budget is equivalent to the divergence of the vertically integrated water vapor flux. Figure 1 shows climatology of vertically integrated water vapor flux (surface-100 hPa) and its divergence in summer (JJA) from 1979 to 2010 derived from JRA-55 reanalysis datasets. The net freshwater flux (E-P) is inhomogeneous in TCZ. Water vapor convergence is observed in the northeast part of the TCZ with moisture divergence in central and southwest. The Indian Peninsula, the southern foothills of the Himalayas, the Indo-China Peninsula and tropical

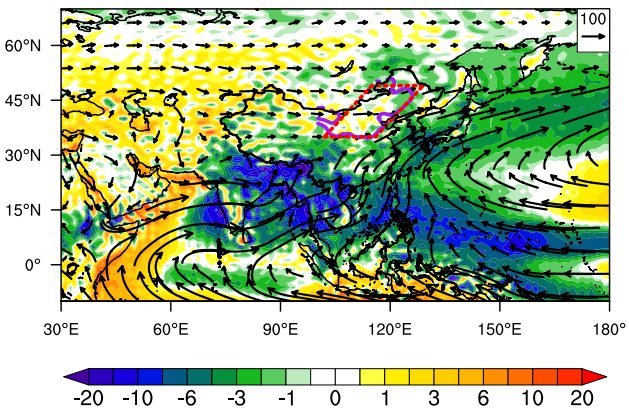

Fig. 1 Vertically integrated (surface − 100 hPa) water vapor flux (arrows, units: kg m^{-1} s^{-1}) and its divergence (contour, units: 10^{-5} kg m^{-2} s^{-1}) in TCZ during June–August of 1979–2010 derived from JRA-55. Geographical position of summer TCZ (thick purple solid line) identified with SM_AI by Wang et al. (2021) and its simplified boundary (red dashed line)

western Pacific are characterized by strong water vapor flux convergence, leading to abundant summer precipitation. The western part of Eurasia is subjected to moisture divergence, with positive net water vapor flux and greater evaporation than precipitation. According to the water vapor transport field, there are three possible transport pathways of moisture during summer in TCZ. First, the mid-latitude westerlies dominate moisture transport over TCZ. Second, southwesterly circulation brings moisture from the Arabian Sea and the Bay of Bengal as well. Third, the anticyclone fetches warm and moist air from the tropical Pacific Ocean and South China Sea to TCZ, along the west margin of the western Pacific high.

In this study, we explore moisture supply for summer precipitation in TCZ from June to August. Given the average residence time of water vapor in the atmosphere is 10-days (Numaguti 1999), we think that May 21 is a more suitable date to start the simulation so the moisture source during the first ten days of June can be traced. Therefore, FLEXPART_10.4v ran forward in time every summer from May 21 to August 31 of 1979–2010 using the domain-filling mode, with 1,000,000 particles all released globally in the beginning. The model output includes three-dimensional position (latitude, longitude, and altitude), temperature, specific humidity, air density, and mass of each air particle, recorded at 6-hourly intervals.

2.3 E–P and P diagnostics

The Lagrangian analog (Stohl and James 2004) is applied to diagnose surface freshwater budget, which equals to evaporation (E) minus precipitation (P). For a particle, the net rate of change of the water vapor content is

$$e - p = m\frac{\mathrm{d}q}{\mathrm{d}t} \tag{1}$$

where e and p are the rates of moisture uptake and release along the trajectory, respectively. m is the mass of the particle. q is the specific humidity, and dq/dt is the change of specific humidity with time. Giving that when rain falls, it normally clearly exceeds evaporation. Stohl and James (2004) suggested that we can assume that e and p cannot coexist in the same location at the same time. That means there is only uptake of moisture ($e > 0$, $p = 0$) happening when $\mathrm{d}q/\mathrm{d}t > 0$ and vice versa. However, a threshold of specific humidity change of $0.2g/kg$ per 6-hours instead of 0 is used to determine moisture uptake ($\mathrm{d}q > 0.2g/kg$) or release ($\mathrm{d}q < -0.2g/kg$) in order to reduce errors caused by numerical noise and keeps the analysis computationally feasible (James et al. 2004; Sodemann et al. 2008; Huang and Cui 2015).

The surface freshwater flux in an area A becomes the moisture changes of all particles in the atmospheric column over A

$$E - P = \frac{\sum_{k=1}^{k=K}(e-p)}{A} = \frac{\sum_{k=1}^{k=K} m\frac{dq}{dt}}{A} \tag{2}$$

where K is the total number of particles in the atmospheric column over A. In this study, E–P budgets are calculated on a 1°×1° grid.

Theoretically, Eq. (2) can diagnose E–P as a whole, but not E or P individually. However, given the fact that when rain falls, it normally clearly exceeds evaporation, and thus similar assumption can be made that E and P cannot coexist in the same location at the same time (Stohl and James 2004). For individual time steps, E_i =E–P when E–P > 0, or precipitation P_i =E–P when E–P < 0. Therefore, the precipitation over time period can be formulated as:

$$\overline{P} = \sum_{i=1}^{i=n} P_i \tag{3}$$

Equations (1) and (3) are based on the same assumptions that all moisture decrease is due to precipitation and that precipitation falls immediately (James et al. 2004; Sodemann et al. 2008).

2.4 Moisture contribution

There are 2 possible activities and 3 kinds of locations in the air particle's path as shown in Fig. 2a. In order to quantify the contribution of each evaporation location along a trajectory to the precipitation at the target location, Sodemann et al. (2008) introduced a 'moisture source attribution method'. Based on that, Sun and Wang (2014) developed a "areal source–receptor attribution method" to calculate the contribution of an examined source region to the total precipitation in target region. Considering the subject explored in this study, we adopt the latter and make some minor modifications here. Before we started select target air particles, analysis of observed daily precipitation data shows that precipitation occurred every day in the target region during the study period. It makes our calculation much easier by skipping the step of marking rainy days. Instead of tracing back 10 days, the whole simulated time is considered to avoid discrepancy caused by recycling time of moisture over different regions. Detailed processing procedures are presented as follows:

1) Find all air particles that have moisture released ($\mathrm{d}q < -0.2g/\mathrm{kg}$) from June 1 to August 31 in the target regions (TR) from model output files and calculate the total moisture release Rtotal (unit: kg).

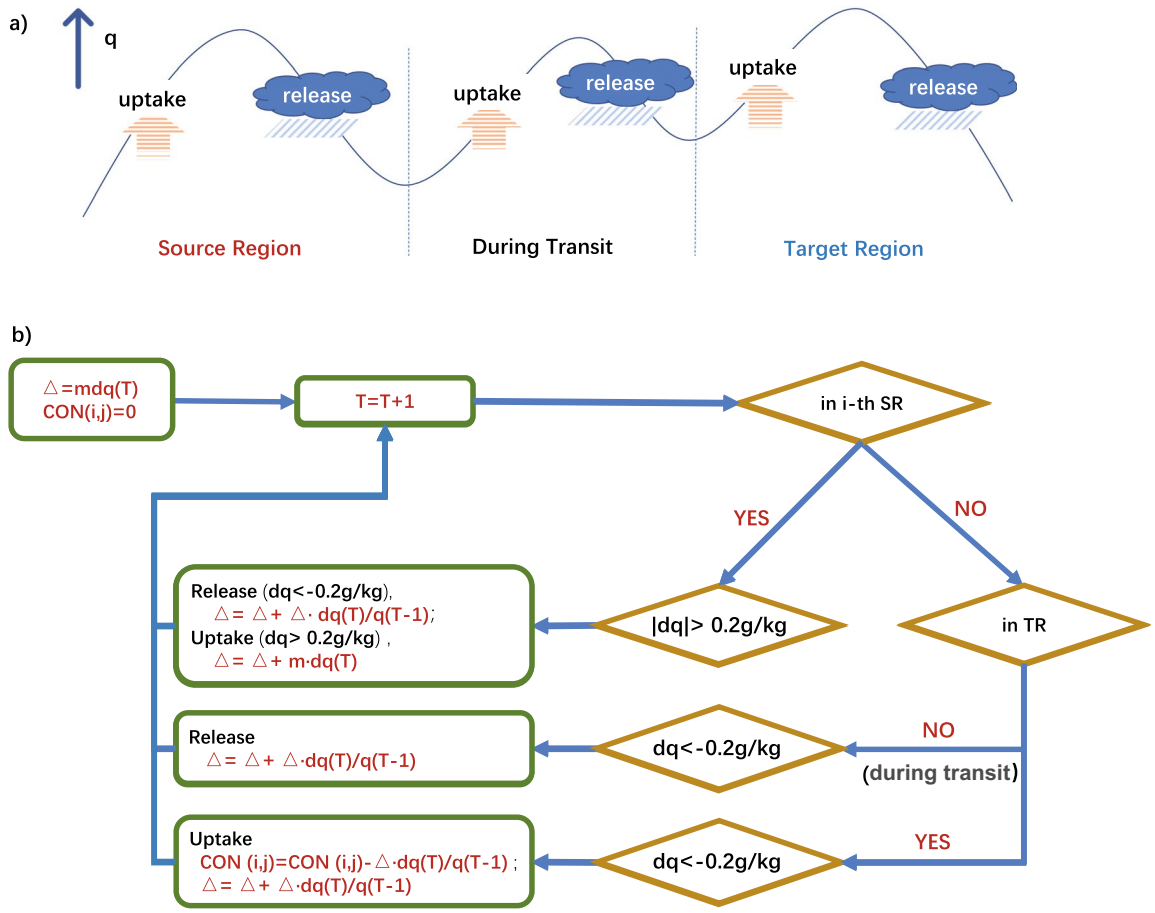

Fig. 2 **a** Possible situations an air particle may occur before it reaches target region. **b** Calculation process of absolute moisture contribution of the j-th air particle uptake from i-th source region to the precipitation in the target region. dq = q(T)–(T–1), unit: kg/kg; △: water vapor that is uptake in i-th source region, unit: kg; CON(i, j): accumulated water vapor from i-th source region released in the target area by air block i, unit: kg

2) Among the air particles selected in step 1, for the i-th examined source region (SR), its contribution to the target region is referred as CON(i). Find all the air particles passing over this region that have uptake of moisture from there ($dq > 0.2g/\mathrm{kg}$).

3) For j-th air parcel selected in step 2, the computation of its moisture contribution from the i-th SR to precipitation in TCZ (CON(i,j) ,unit: kg) is shown in Fig. 2b. All possible situations should be considered along its way to the target region(Fig. 2a).To begin with, find the first (forward in time) time (T) moisture uptake over the i-th SR, and the moisture mass from i-th SR (Δ, unit : kg) in this particle at present is $m$dq(T) with present moisture contribution (CON(i,j)) equals to 0. The following calculations are detailed in Fig. 2b.

4) Repeat step 3 on all particles selected in step 2. The absolute (CON(i), unit: kg) and relative moisture contribution (RCON(i), unit: %) from i-th SR can be given by :

$$CON_{(i)} = \sum_{j=0}^{j=J} CON_{(i,j)} \tag{4}$$

$$RCON_{(i)} = \frac{CON_{(i)}}{Rtotal} \times 100\% \tag{5}$$

where J is the total number of air particles of step 2.

3 Results

3.1 Lagrangian precipitation estimate

Before detecting the moisture sources for TCZ, it is of great importance to test the performance of simulated Lagrangian precipitation in TCZ by FLEXPART_10.4 V. Previous studies have proved its capability in reproducing the

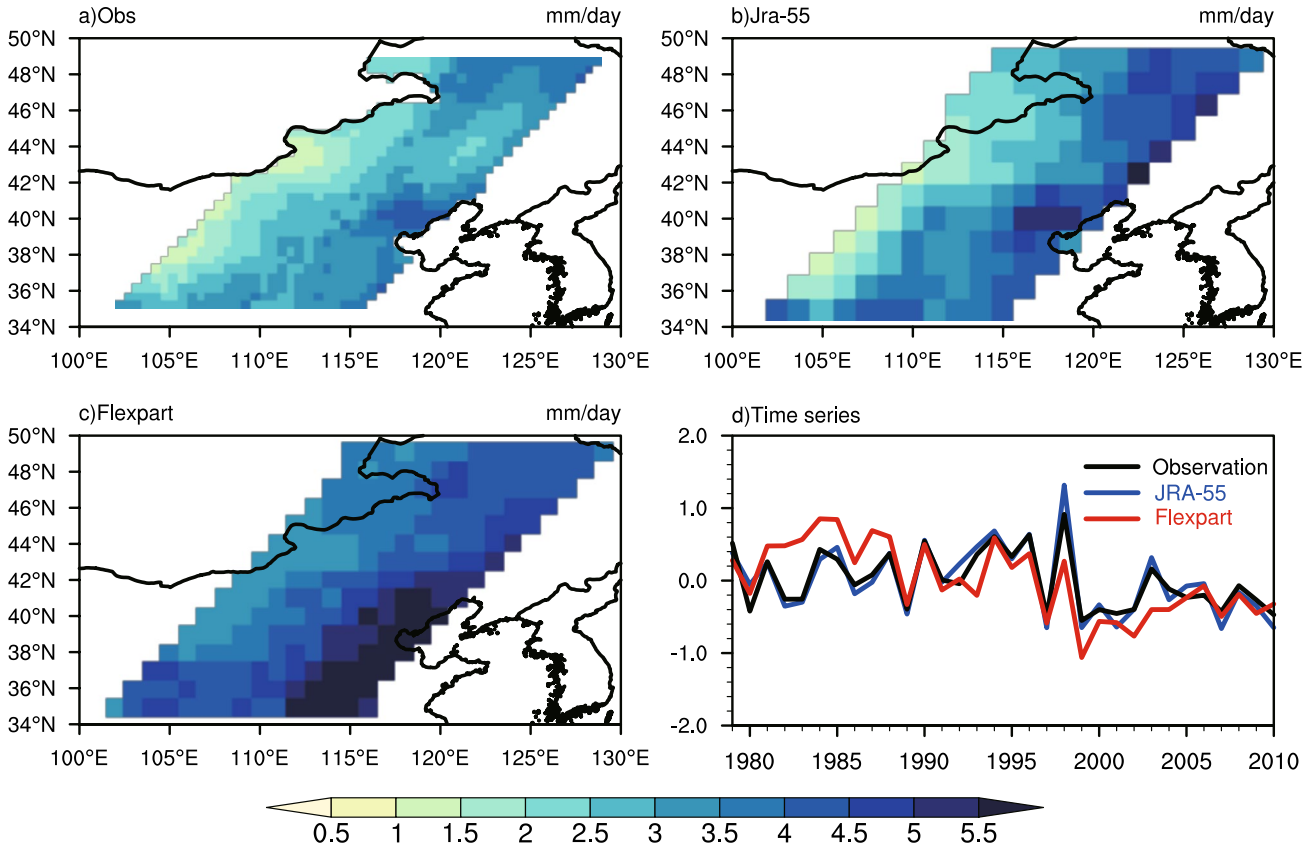

Fig. 3 Spatial distribution of the climatological summer (June–August) precipitation (units: mm/day) during 1979–2010 from **a** observation, **b** JRA-55, and **c** simulated results of Flexpart10.4, as well as corresponding time series of their precipitation anomalies (**d**)

observed precipitation. For example, James et al. (2004) compared results of moisture fluxes and precipitation of 2002 obtained with the Lagrangian and Eulerian method. Their results agreed well with each other, and both agreed well with observed precipitation patterns and shortrange precipitation forecasts. Sodemann et al. (2008) also suggested the rationality of considering the Lagrangian precipitation estimates a valid approximation over Greenland.

In this study, we also compared our results from FLEXPART_10.4v model with reanalysis data from JRA-55 and observation daily precipitation from National Meteorological Information Center. The climatic mean summer (JJA) precipitation calculated from the model output in TCZ during 1979–2010 is 4.35 mm/day, while those derived from observation and JRA-55 are 2.81 mm/day and 3.37 mm/day, respectively. Compared with observation and reanalysis data, Lagrangian method tends to overestimate the precipitation because of diagnosis of extra precipitation upon cloud formation (Stohl and James 2004). Nevertheless, the spatial pattern of the summer precipitation over TCZ is well reproduced, with larger amounts in the southeast than in the northwest (Fig. 3a-c). Time series of precipitation anomalies simulated by the model are in good agreement with the reanalysis data and observation data (Fig. 3d). The Pearson correlation coefficients between the model output and reanalysis and observed datasets are 0.63 and 0.7 with significance above 95% confidence level. Overall, the model simulation is capable of reflecting the spatial distribution and variation of summer precipitation in TCZ during 1979–2010.

3.2 Trajectories and E–P diagnosis

The average residence time of water vapor in the atmosphere is 10-days according to previous studies (Numaguti 1999). Air particles that released water vapor in TCZ from June 1 to August 31 during 1979–2010 were selected and traced back 10 days (240 h) for E–P diagnosis to find the moisture source-sink relationship for summer precipitation in TCZ. Over 8 million trajectories were selected during these 32 years, since one particle may release moisture more than once in TCZ and so can be selected multiple times. The k-means++ clustering algorithm is applied to agglomerate these numerous trajectories (Dorling et al. 1992; Arthur and Vassilvitskii 2007; Thinsungnoen et al. 2015). To select the optimal cluster numbers, the elbow method is used by

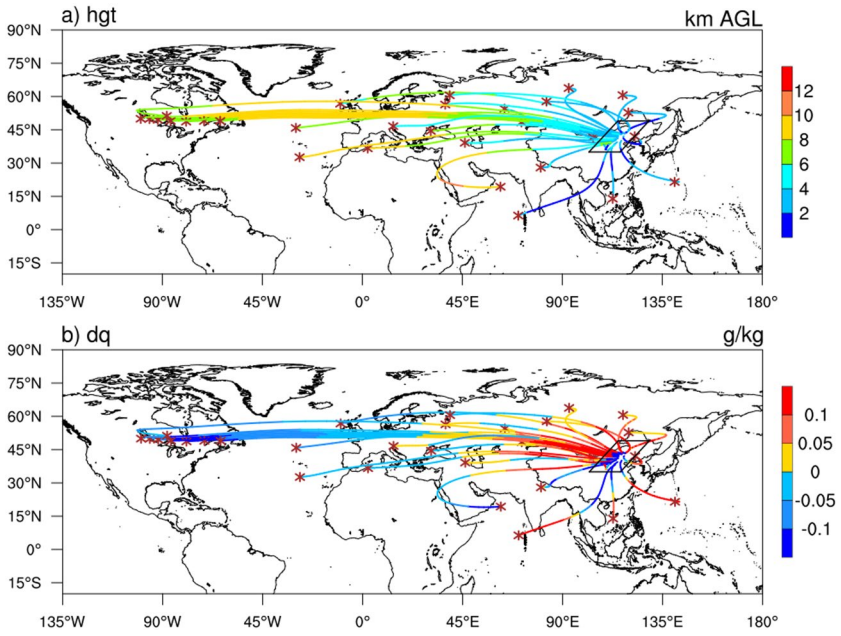

Fig. 4 Cluster mean trajectories (number: 30) of particles for the 10 days prior to reaching TCZ in the summers of 1979–2010. **a**) The trajectories are colored according to the altitudes above ground level (units: km AGL). **b** colored according to the specific humility change (dq, units: g/kg). The target region TCZ is expressed by the polygon in bold black

finding the elbow point in the SSE (Sum of Square Errors) curve (figure not shown). As a result, the cluster number of 30 is finally chosen. It is worth noting that the cluster analysis can only sketch the trajectories for target air particles, and the density of these cluster trajectories can't reflect the intensity of water vapor transport. Figure 4 shows 30 cluster mean trajectories of particles colored with average height above ground level (AGL) and specific humidity change of the particles for the 10 days prior to reaching TCZ during the summers of 1979–2010. The air parcels over TCZ during summer can be divided into 4 main paths: (1) air blocks traveling along the warm anticyclone in the upper troposphere over the Qinghai-Tibet Plateau and North Africa, above 8 km AGL; (2) Air particles from the upper atmospheric layers over the North Atlantic, mostly above 8 km AGL, travel along the latitudes over Europe and Central Asia and reach the TCZ; 3)the air masses from higher latitudes in northern Asia heading towards TCZ (2–6 km AGL). 4) lower air particles, mainly below 2 km AGL, entering TCZ from North Indian Ocean or West Pacific Ocean via East Asia. Note that for particles comes from first three paths, it is not until they reached Eurasia that they begin uptake water vapor. In the meanwhile, particles originating from North India Ocean and West Pacific Ocean tend to loss moisture when they enter the land. The specific humidity changes of particles indicate that the direct moisture contribution from oceans may be undermined because of the precipitation over long distances, which is also proved by the results shown in Sect. 3.4.

Although the cluster trajectories offer detailed moisture transport paths and water vapor change along the way, it is not adequate to identify water vapor sources accurately

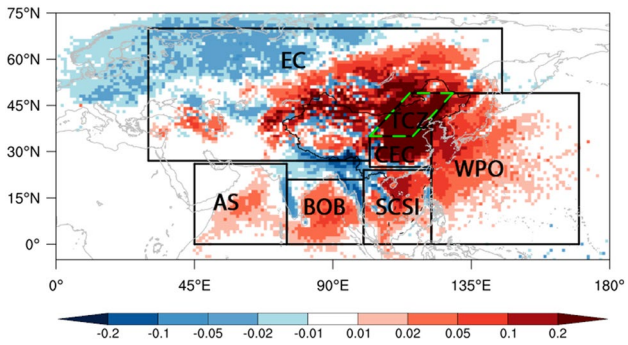

Fig. 5 Mean E–P (unit: mm/day) of target-bound air parcels in 1–10 days before reaching TCZ during June–August of 1979–2010. Seven moisture source regions for TCZ are identified, which are most of Eurasia continent in northwest of the TCZ (EC), central-eastern China (CEC), western Pacific Ocean (WPO), South China Sea and Indonesia (SCSI), Bay of Bengal (BOB), Arabian Sea (AS) and local evaporation (TCZ)

only based on that. To better identify the source-receptor relation, the averaged E–P budget of all selected trajectories is calculated (Sun and Wang 2015; Peng et al. 2020). Figure 5 shows the mean E–P of all particles selected for the 10-day period prior to reaching there during the summer of 1979–2010. The positive E–P value can be recognized as a moisture source region where total moisture uptake is stronger than release, while the negative value suggests a moisture sink that involves a net release of moisture. There are approximately seven source regions for the target region, which are most of Eurasia continent to the northwest of the TCZ (EC), central-eastern China (CEC), western Pacific Ocean (WPO), South China Sea and Indonesia (SCSI), Bay

of Bengal (BOB), Arabian Sea (AS) and local evaporation (TCZ). The southwest of Indian Peninsula, the southern foothills of the Himalayas and the Indo-China Peninsula are water vapor sink areas, consistent with the strong convergence area in Fig. 1, which can be explained by the large terrain blocking the Indian summer monsoon. Furthermore, the northwest Eurasia is also featured by negative E–P value, which means air parcels passing this area also encounter a large amount of moisture release.

3.3 Quantification of moisture contribution from source regions

The relative moisture contributions of 7 source regions selected in Sect. 3.2 to the summer precipitation of TCZ during 1979–2010 are calculated with the method described in Sect. 2.4. The moisture uptake from the source regions (Uptake) by the target air particles that have released water vapor during summer in TCZ was divided into three parts along its way to the target domain(Sun and Wang 2014, 2015): moisture released before reaching TCZ (Loss), the part that reached TCZ but was not released (Unreleased), and water vapor that reached and released in the TCZ, the one making an actual contribution to precipitation over TCZ (Contribution). Figure 6 shows ratios of water vapor uptake in each source region to total TCZ water vapor release in summer, as well as moisture contributions from selected source regions, loss en-route and unreleased moisture. The seven examined source regions contribute 95.02% of water supply, explaining most of the water vapor that contributes to summer precipitation in TCZ from 1979 to 2010. The continental moisture from TCZ, CEC and EC accounts for 81.34% of the summertime total moisture release, while the oceanic moisture from WPO, SCSI, BOB and AS only accounts for 13.67% because of a large amount of moisture loss during transit. Local evaporation (32.58%) and Eurasia (32.14%) provides the most water vapor for summer precipitation in TCZ among all source regions. In addition, evaporation over central and eastern China is also accounting for 16.62% moisture contribution. Even without taking into account of actual contribution to precipitation, continental moisture is still the primary source of water vapor over the transition zone (Unreleased + Contribution), bringing more moisture (156.41%) to the TCZ than ocean (27.65%), which stresses the importance of terrestrial hydrological recycling for moisture supply of TCZ during summer. However, water vapor uptake (442.87%) in EC loss a lot (379.04%) during the transport compared with TCZ and CEC. Despite a large amount of water vapor uptake (323.18%), western Pacific Ocean is only responsible for 8.58% of water vapor supply for summer precipitation of TCZ, which is about two thirds of moisture contribution that comes from the ocean. Water vapor from SCSI, BOB and AS only account for 2.99%, 1.4% and 0.71% moisture released in TCZ, respectively.

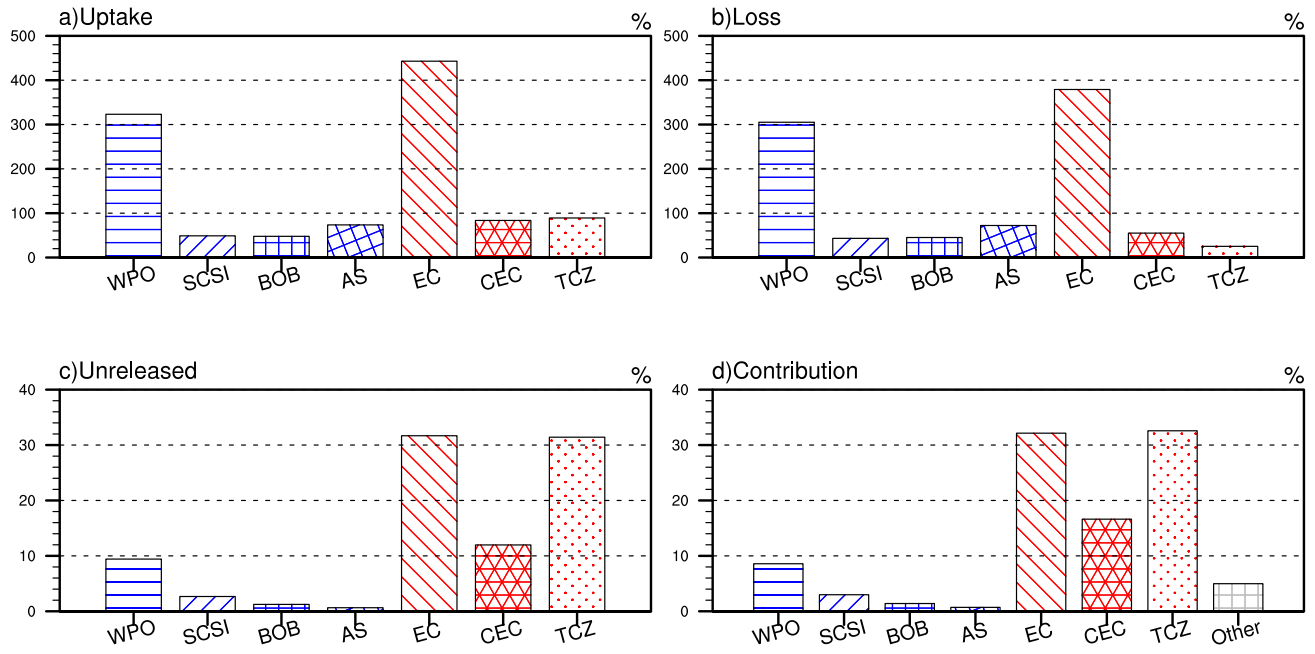

Fig. 6 **a** The ratios of the moisture uptake from the seven examined source areas and other area to the total moisture release in the TCZ during June-August in 1979–2010 (unit: %), which consist of three parts: the part lost en-route (**b**), the part that reaches the target domain but is not released (**c**), and the part that is released over the target domain and contributes to summer rainfall (**d**)

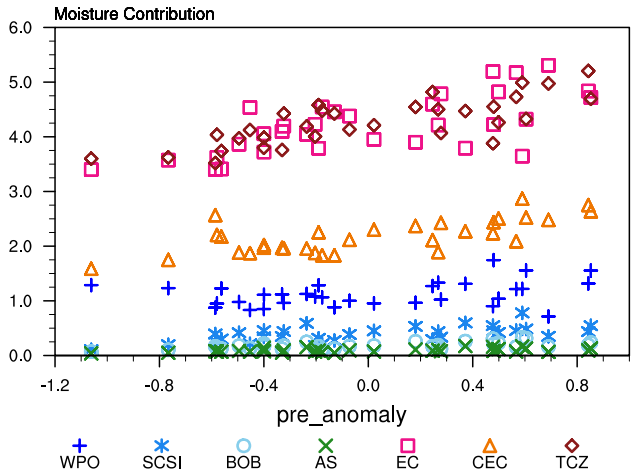

Fig. 7 Scatter diagram of model simulated summer rainfall (units: mm/day) during 1979–2010 versus moisture contribution (units: 10^{14} kg) in TCZ from seven resource regions

3.4 The role of different source regions in variation of summer precipitation in TCZ

Results above shows the climatological contributions of source regions. In the following, the roles of different moisture source regions in summer rainfall variation in TCZ are investigated because of the strong climate fluctuation in this region (Wang et al. 2021). Figure 7 shows the scatter of vapor contribution of each region versus summer precipitation during 1979–2010. Generally, as precipitation increase, the contributions from all 7 source regions exhibit an upward tendency, especially in the land regions (EC, CEC and local evaporation), which are confirmed by the regression results in Table 1. EC and local evaporation are not only one of the major moisture suppliers, but also exerts major effects on the sensitivity of precipitation in TCZ. Among the four ocean sources, WPO contributes the most moisture. However, when rainfall is relatively small, water vapor from Western Pacific remains roughly constant irrespective of summer precipitation in TCZ, unlike other source regions.

For better understanding of which source region should take primary responsibility for the summer rainfall variation in TCZ, we also conduct linear regression and correlation analyses of water vapor uptake amount and absolute moisture contributions from 7 source regions against summer precipitation simulated by the model (Table 1). The correlation coefficient between the sum of water vapor released in the target region from all selected source and precipitation in the transition zone is 0.97, which means moisture contributions from all selected source areas can well capture precipitation changes. All correlation scores in the Table 1 show positive correlation between water vapor from 7 source regions and precipitation, with correlation coefficient (r) varying from 0.11 to 0.81, while regression coefficient (k) varying from 0.16 to 9.81. The correlation between moisture release from local evaporation and summer precipitation is highest with r = 0.78 and k = 0.66. Regression coefficient of moisture contribution from EC (k = 0.73) is greater than those from other regions, meaning that TCZ precipitation variability is most sensitive to changes in EC. Although moisture contribution from CEC has a good correlation with summer rainfall in TCZ (r = 0.72), correlation coefficient and regression coefficient between uptake moisture amount and simulated summer rainfall both failed the significant test. It indicates the moisture absorbed in CEC are more likely fall out during the transit. As for WPO, the correlation and regression coefficient of moisture contribution are 0.15 and 0.33, while those of moisture uptake over WPO are 4.16 and 0.69. It shows that moisture uptake because of the evaporation over this area is closely related to summer precipitation in TCZ, although the impact of direct contribution is relatively small. The possible reason is that the absorbed water falls in other places and indirectly contributes to TCZ through the re-absorption after precipitation on the way. The contributions from other three oceanic source regions SCSI, BOB and AS, are small but significantly correlated with summer rainfall in TCZ, with r = 0.61, 0.6 and 0.49, respectively.

We also select wet/dry years of summer in TCZ based on normalized summer precipitation above 0.75 standard deviation (Table 2) to further explore how moisture contribution changes from 7 regions. The average moisture contributions from different regions in dry and wet years to summer precipitation in TCZ are compared in Fig. 8, along with total

Table 1 Pearson linear correlation coefficients (r) and linear regression coefficients (k) and between precipitation in TCZ and moisture release (units,10^{14} kg) from source regions and the total moisture uptake amount over selected source regions

		EC	CEC	WPO	SCSI	BOB	AS	TCZ	Total
Uptake	k	9.81**	0.16	4.16**	1.24**	0.88**	1.04**	1.24**	18.52**
	r	0.76**	0.11	0.69**	0.63**	0.5**	0.4**	0.81**	0.98**
Contribution	k	0.73**	0.44**	0.15*	0.17**	0.08**	0.03**	0.66**	2.38**
	r	0.69**	0.72**	0.33*	0.61**	0.6**	0.49**	0.78**	0.97**

*Passing the significant level of 0.1

**Passing the significant level of 0.05

Table 2 Wet years and dry years selected according to summer precipitation during 1979–2010

	year
Dry year	1981/1982/1983/1984/1985/1987/1988/1990/1994
Wet year	1997/1999/2000/2001/2002/2003/2004/2007/2009

water vapor uptake and loss en-route and unreleased water vapor. Compared with dry years, the moisture contribution from each source region increased uniformly and significantly in wet years, leading to the ample precipitation. The water vapor released in TCZ from land has increased much more than that from the sea (Fig. 8b). Therefore, moisture recycled from land takes more responsibility for variation of summer precipitation. CEC, as one of the main sources of water vapor, has the smallest increment in moisture uptake during wet years, but its contribution to the TCZ is still appreciable because of its little change in moisture loss during transit. This is also the case for local evaporation in TCZ. Although the absorption of water vapor increases in WPO during wet years, the moisture is also enhanced concordantly. Therefore, the net effect of released moisture from WPO is not as great as that of land sources.

In general, Among the seven regions, direct moisture contributions from land regions have greater influence to the summer rainfall variation of TCZ than those from oceanic regions, especially recycling from local evaporation. In addition, analysis of uptake moisture also indicates the importance of evaporation in WPO in shaping dry-wet condition of TCZ during summer.

3.5 The qualified impact of summer monsoon system and the mid-latitude westerlies

There have been evidence showing that summer rainfall in TCZ is mainly modulated by monsoon circulation and mid-latitude westerlies (Simmonds et al. 1999; Huang et al. 2011). However, the complicate interaction between the westerlies induced precipitation and monsoon rainfall (Qian et al. 2009) makes it hard to determine the dominant system influencing wet-dry condition of TCZ based on Eulerian model. Here, the Lagrange method provides us a new perspective to address this issue by quantifying the relative moisture contribution of each system. Among the seven regions, water vapor from CEC, WPO, SCSI, AS and BOB is linked to summer monsoon systems, while EC is tied to

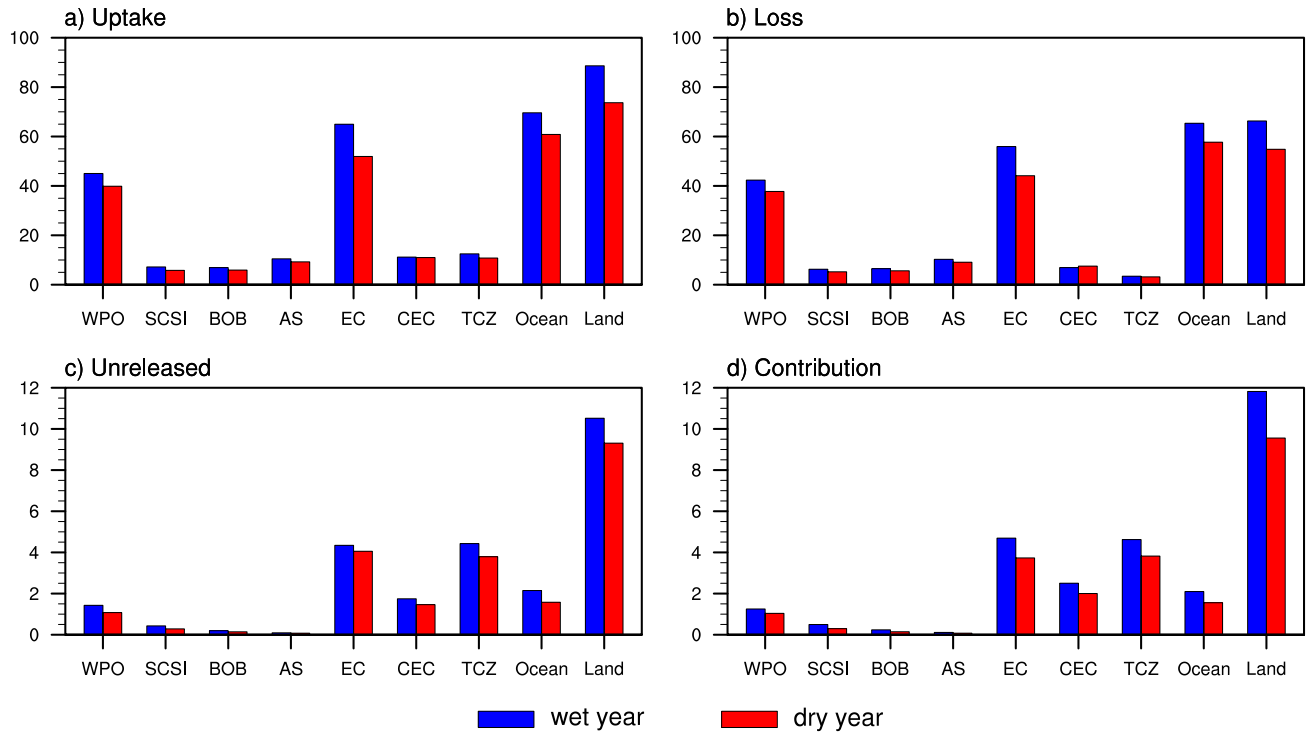

Fig. 8 Moisture contributions to summer precipitation during 1979–2010 from seven source regions (units:10^{14} kg), as well as **b** total moisture uptake in source regions, **c** loss during transport, and **d** unreleased moisture

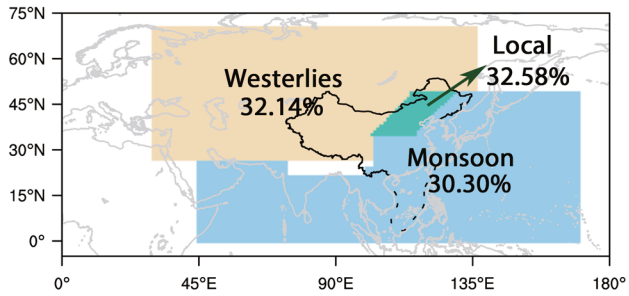

Fig. 9 Three dominated systems in moisture source regions of TCZ in summer during 1979–2010 and their climatological relative moisture contribution (units:%)

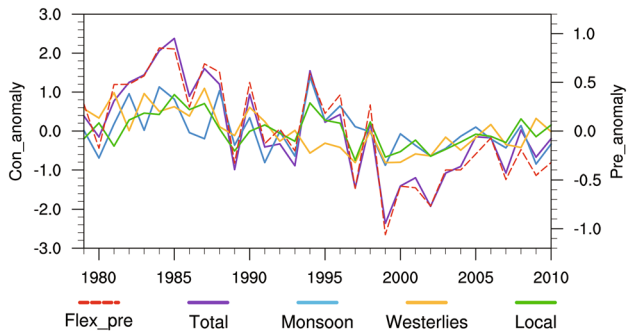

Fig. 10 Time series of summer precipitation anomalies (JJA) (units:mm/day) in TCZ during 1979–2010 simulated by FLEXPART (red dashed line), as well as moisture contribution anomalies (units: 10^{14} kg) related with monsoon system (blue solid line), westerlies(yellow solid line), local evaporation (green solid line) and total contribution of all three systems(green solid line)

the mid-latitude westerlies as demonstrated in Fig. 9. Monsoon circulation dominated area contribute 30.3% moisture for summer rainfall in TCZ, summed by contributions from CEC, WPO, SCSI, AS and BOB. It is important to point out that the summer monsoon systems in this study include both east Asia summer monsoon and India summer monsoon. Summer rainfall caused by moisture from the area controlled by westerlies (EC) is 32.14%, while the local evaporation contributes 32.58%. Figure 10 shows time series of summer precipitation anomalies in TCZ during 1979–2010 simulated by FLEXPART, as well as moisture contribution anomalies of different systems. The variation of total contribution of all three systems is well agree with simulated precipitation with correlation coefficient r = 0.96 (Fig. 11a) which is significant at the 95% level. The moisture contributions from summer monsoon and westerlies don't agree with each other well, and shows no significant linear correlation with correlation coefficient r = 0.11.

Wet/dry condition in TCZ during summer is featured by strong inter-annual oscillation(Wang et al. 2021) which is also the time scale we focus on in this article. Therefore, we applied Fast Fourier transform filter on lagrangian precipitation sequences and moisture contributions with only inter-annual oscillation components retained. To illuminate how moisture contribution related with summer monsoon, westerlies and local evaporation influence inter-annual variation of summer precipitation, both linear regression and correlation analyses of annual component of moisture contributions against corresponding summer precipitation are conducted. And the results are shown in Fig. 11. The correlation coefficient between summer rainfall and total moisture release is 0.96, which means that variation of total moisture of selected region well explained the inter-annual fluctuation of summer rainfall in TCZ. The regression coefficients of moisture contribution from monsoon system, the westerlies and local evaporation are 1.11 ,0.47 and 0.59, respectively, with corresponding correlation coefficients are, 0.67, 0.44, 0.63, all of which pass the significant test with the significant level of 0.05. Overall, the released moisture conveyed by the monsoon system plays more important part in inter-annual variation of summer rainfall in TCZ, followed by local evaporation and mid-latitude westerlies.

4 Concluding remarks

In this study, we reproduced Lagrangian precipitation of TCZ in summer during 1979–2010 using the output of FLEXPART_10.4v. Compared with observation precipitation and reanalyzed data, the simulated precipitation is overestimated without considering the condensation water. However, results still well reproduced spatial distribution characteristics of summer precipitation in TCZ and its temporal variation.

Air particles that reached TCZ during summer mainly travel through four paths. As for the air blocks in the upper troposphere, plenty of them come from the North Atlantic to TCZ along with the mid-latitude westerlies. Some of them travel along the warm anticyclone in the upper troposphere over the Qinghai-Tibet Plateau and North Africa. Some of the air parcels in the middle and lower layers over TCZ come from regions of northern Asia and higher latitudes, with others from the Indian Ocean and the western Pacific Ocean.

Seven moisture source regions are identified based on E–P diagnosis, which are responsible for over 95% moisture contribution to summer precipitation over TCZ during 1979–2010. The moisture contribution to summer precipitation in TCZ from land region is much greater than that from the ocean. Evaporation from local and Eurasian continent is the major moisture sources for precipitation over TCZ, followed by central and eastern China. Most of the water vapor in selected regions loss in transit, especially for oceanic regions. Although there is a mass of moisture taken up in WPO, only about 8% of the water vapor contributed to

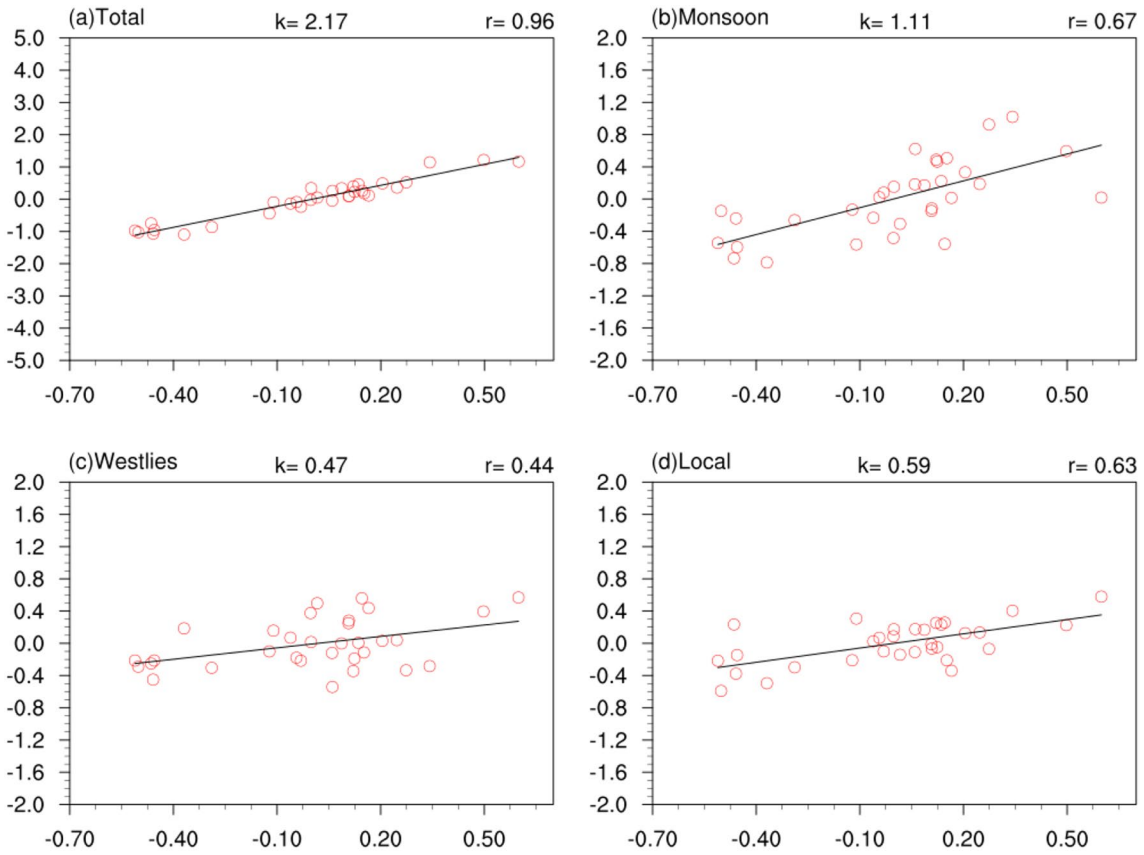

Fig. 11 Scatter plot of inter-annual variation of lagrangeian precipitation during Jun-Aug in TCZ versus total moisture release anomalies (**a**) and moisture contributions from regions dominated by summer monsoon system (**b**), westerlies (**c**), local evaporation (**d**), with linear regression line superimposed (black line). The X-axis is normalized inter-annual components of area average summer precipitation of TCZ, and Y-axis represents interannual variation of moisture contributions anormalies from different climate systems. The values of k and r are the regression and correlation coefficients, respectively. All passed significant level of 0.05

summer precipitation in TCZ comes from this region. Correlation analysis also indicates that WPO may have indirect impact on summer precipitation in TCZ. Moisture increment between wet years and dry years from land is much greater than that from ocean, indicating the importance of terrestrial hydrological cycle in the inter-annual variation of summer rainfall of TCZ.

The Lagrange method makes it possible to quantify the influences of different systems to the summer precipitation in TCZ from the perspective of water vapor supply. Moisture contributions from westerlies, summer monsoon systems and local evaporation are distinguished according to the dominant system of water vapor source regions. The amounts of moisture conveyed by summer monsoon systems which consists of moisture from WPO, SCSI, BOB, AS and CEC, westerlies (EC) and local evaporation results in quite similar, which all contribute around 30% moisture to summer rainfall. However, the regression analysis shows a closer connection between summer precipitation in TCZ and summer monsoon systems, compared with the mid-high latitude systems. The results indicates that the summer monsoon plays a more important role on the interannual variation of precipitation in TCZ followed by local evaporation and westerlies.

Acknowledgements This work was supported by the National Natural Science Foundation of China Grants Nos. 41875115, 41961144016, 42175041 and 41831175, STEP (2019QZKK0102) and Key Deployment Project of Centre for Ocean Mega-Research of Science, Chinese Academy of Sciences (COMS2019Q03).

Data Availability The FLEXPART model is driving by NCEP–CFSR 6-hourly forecast data dataset, which can be retrieved from http://rda.ucar.edu/datasets/ds093.0/. Japanese 55-year Reanalysis dataset (JRA-55), constructed by the Japan Meteorological Agency, are also available online (http://search.diasjp.net/en/dataset/JRA55). The daily observation precipitation data used in this study is provided by the National Meteorological Information Center of the China Meteorological Administration (CMA; https://data.cma.cn/)

Declarartions

Conflict of interest The authors declare that they have no conflict of interest.

References

Bin C, Xiang-De X, Tianliang Z (2013) Main moisture sources affecting lower Yangtze River Basin in boreal summers during 2004–2009. Int J Climatol 33(4):1035–1046

Chen J, Wei H, Jin LY, Chen JH, Chen SQ, Chen FH (2018) A climatological northern boundary index for the East Asian summer monsoon and its interannual variability. Sci China-Earth Sci 61(1):13–22

Chen B, Zhang W, Yang S, Xu XD (2019) Identifying and contrasting the sources of the water vapor reaching the subregions of the Tibetan Plateau during the wet season. Clim Dyn 53(11):6891–6907

Chen W, Wang L, Feng J, Wen ZP, Ma TJ, Yang XQ, Wang CH (2019) Recent progress in studies of the variabilities and mechanisms of the East Asian Monsoon in a changing climate. Adv Atmos Sci 36(9):887–901

Dorling SR, Davies TD, Pierce CE (1992) Cluster-analysis - a technique for estimating the synoptic meteorological controls on air and precipitation chemistry - method and applications. Atmos Environ Part a General Top 26(14):2575–2581

Hao Y, Zhihong J, Zhengyu L, Qiang Z (2014) Analysis of climatic characteristics of water vapor transport based on the Lagrangian method: a comparison between Meiyu in the Yangtze – Huaihe River region and the Huaibei rainy season. Chin J Atmos Sci 38(5):965–973

Harada Y, Kamahori H, Kobayashi C, Endo H, Kobayashi S, Ota Y, Onoda H, Onogi K, Miyaoka K, Takahashi K (2016) The JRA-55 reanalysis: representation of atmospheric circulation and climate variability. J Meteorol Soc Jpn 94(3):269–302

He C, Zhou W (2020) Different enhancement of the East Asian Summer Monsoon under Global Warming and Interglacial Epochs Simulated by CMIP6 Models: role of the subtropical high. J Clim 33(22):9721–9733

Huang YJ, Cui XP (2015) Moisture sources of an extreme precipitation event in Sichuan, China, based on the Lagrangian method. Atmos Sci Lett 16(2):177–183

Huang G, Liu Y, Huang RH (2011) The Interannual Variability of Summer Rainfall in the Arid and Semiarid Regions of Northern China and Its Association with the Northern Hemisphere Circumglobal Teleconnection. Adv Atmos Sci 28(2):257–268

Huang R, Liu Y, Feng T (2012) Interdecadal change of summer precipitation over Eastern China around the late-1990s and associated circulation anomalies, internal dynamical causes. Chin Sci Bull 58(12):1339–1349

Huang J, Li Y, Fu C, Chen F, Fu Q, Dai A, Shinoda M, Ma Z, Guo W, Li Z, Zhang L, Liu Y, Yu H, He Y, Xie Y, Guan X, Ji M, Lin L, Wang S, Yan H, Wang G (2017) Dryland climate change: recent progress and challenges. Rev Geophys 55(3):719–778

Huang JP, Ma JR, Guan XD, Li Y, He YL (2019) Progress in semi-arid climate change studies in China. Adv Atmos Sci 36(9):922–937

Huang JP, Zhang GL, Zhang YT, Guan XD, Wei Y, Guo RX (2020) Global desertification vulnerability to climate change and human activities. Land Degrad Dev 31(11):1380–1391

James P, Stohl A, Spichtinger N, Eckhardt S, Forster C (2004) Climatological aspects of the extreme European rainfall of August 2002 and a trajectory method for estimating the associated evaporative source regions. Nat Hazards Earth Syst Sci 4(5–6):733–746

Kobayashi S, Ota Y, Harada Y, Ebita A, Moriya M, Onoda H, Onogi K, Kamahori H, Kobayashi C, Endo H, Miyaoka K, Takahashi K (2015) The JRA-55 reanalysis: general specifications and basic characteristics. J Meteorol Soc Jpn 93(1):5–48

Li Y, Huang JP, Ji MX, Ran JJ (2015) Dryland expansion in northern China from 1948 to 2008. Adv Atmos Sci 32(6):870–876

Lu W, Jia GS (2013) Fluctuation of farming-pastoral ecotone in association with changing East Asia monsoon climate. Clim Change 119(3–4):747–760

Nieto R, Gimeno L, Trigo RM (2006) A Lagrangian identification of major sources of Sahel moisture. Geophys Res Lett 33(18):L18707

Numaguti A (1999) Origin and recycling processes of precipitating water over the Eurasian continent: Experiments using an atmospheric general circulation model. J Geophys Res-Atmos 104(D2):1957–1972

Oshima K, Tachibana Y, Hiyama T (2015) Climate and year-to-year variability of atmospheric and terrestrial water cycles in the three great Siberian rivers. J Geophys Res-Atmos 120(8):3043–3062

Ou TH, Qian WH (2006) Vegetation variations along the monsoon boundary zone in East Asia. Chin J Geophys-Chin Ed 49(3):698–705

Peng DD, Zhou TJ, Zhang LX (2020) Moisture sources associated with precipitation during dry and wet seasons over Central Asia. J Clim 33(24):10755–10771

Piao JL, Chen W, Wei K, Liu Y, Graf HF, Ahn JB, Pogoreltsev A (2017) An abrupt rainfall decrease over the Asian inland plateau region around 1999 and the possible underlying mechanism. Adv Atmos Sci 34(4):456–468

Pisso I, Sollum E, Grythe H, Kristiansen NI, Cassiani M, Eckhardt S, Arnold D, Morton D, Thompson RL, Zwaaftink CDG, Evangeliou N, Sodemann H, Haimberger L, Henne S, Brunner D, Burkhart JF, Fouilloux A, Brioude J, Philipp A, Seibert P, Stohl A (2019) The Lagrangian particle dispersion model FLEXPART version 10.4. Geosci Model Dev 12(12):4955–4997

Qian WH, Ding T, Hu HR, Lin X, Qin AM (2009) An Overview of Dry-wet Climate Variability among Monsoon-Westerly Regions and the Monsoon Northernmost Marginal Active Zone in China. Adv Atmos Sci 26(4):630–641

Qian CA, Wu ZH, Fu CB, Zhou TJ (2010) On multi-timescale variability of temperature in China in modulated annual cycle reference frame. Adv Atmos Sci 27(5):1169–1182

Salih AAM, Zhang Q, Tjernstrom M (2015) Lagrangian tracing of Sahelian Sudan moisture sources. J Geophys Res-Atmos 120(14):6793–6808

Salih AAM, Zhang Q, Pausata FSR, Tjernstrom M (2016) Sources of Sahelian-Sudan moisture: insights from a moisture-tracing atmospheric model. J Geophys Res-Atmos 121(13):7819–7832

Simmonds I, Bi DH, Hope P (1999) Atmospheric water vapor flux and its association with rainfall over China in summer. J Clim 12(5):1353–1367

Sodemann H, Schwierz C, Wernli H (2008) Interannual variability of Greenland winter precipitation sources: Lagrangian moisture diagnostic and North Atlantic Oscillation influence. J Geophys Res-Atmos 113:D3

Stein AF, Draxler RR, Rolph GD, Stunder BJB, Cohen MD, Ngan F (2015) Noaa's Hysplit atmospheric transport and dispersion modeling system. Bull Am Meteorol Soc 96(12):2059–2077

Stohl A, James P (2004) A Lagrangian analysis of the atmospheric branch of the global water cycle. part I: Method description, validation, and demonstration for the August 2002 flooding in central Europe. J Hydrometeorol 5(4):656–678

Sun B, Wang HJ (2013) Water vapor transport paths and accumulation during widespread snowfall events in Northeastern China. J Clim 26(13):4550–4566

Sun B, Wang HJ (2014) Moisture sources of semiarid grassland in China using the Lagrangian particle model FLEXPART. J Clim 27(6):2457–2474

Sun B, Wang HJ (2015) Analysis of the major atmospheric moisture sources affecting three sub-regions of East China. Int J Climatol 35(9):2243–2257

Trenberth KE, Guillemot CJ (1995) Evaluation of the global atmospheric moisture budget as seen from analyses. J Clim 8(9):2255–2272

Wang L, Chen W (2014) A CMIP5 multimodel projection of future temperature, precipitation, and climatological drought in China. Int J Climatol 34(6):2059–2078

Wang L, Chen W, Huang G, Zeng G (2017) Changes of the transitional climate zone in East Asia: past and future. Clim Dyn 49(4):1463–1477

Wang S, Zuo H, Zhao S, Zhang J, Lu S (2017) How East Asian westerly jet's meridional position affects the summer rainfall in Yangtze-Huaihe River Valley? Clim Dyn 51(11–12):4109–4121

Wang QL, Wang L, Huang G, Piao JL, Chotamonsak C (2021) Temporal and spatial variation of the transitional climate zone in summer during 1961–2018. Int J Climatol 41(3):1633–1648

Xu Y, Zhao P, Si D, Cao L, Wu X, Zhao Y, Liu N (2019) Development and preliminary application of a gridded surface air temperature homogenized dataset for China. Theor Appl Climatol 139(1–2):505–516

Zhao W, Chen W, Chen SF, Nath D, Wang L (2020) Interdecadal change in the impact of North Atlantic SST on August rainfall over the monsoon transitional belt in China around the late 1990s. Theor Appl Climatol 140(1–2):503–516

Zhihong J, Wei R, Zhengyu L, Hao Y (2013) Analysis of Water Vapor transport characteristics during the Meiyu over the Yangzi-Huaihe river valley using theLagrangian method. Acta Meteorol Sin 71(2):295–304

Zhu X, Wu T, Hu G, Wang S, Wu X, Li R, Wang W, Wen A, Ni J, Li X, Hao J (2020) Long-distance atmospheric moisture dominates water budget in permafrost regions of the CentralQinghai-Tibet-plateau. Hydrol Process 34(22):4280–4294

Arthur D, Vassilvitskii S (2007) k-means++: The Advantages of Careful Seeding. Proceedings of the Eighteenth Annual ACM-SIAM Symposium on Discrete Algorithms. Philadelphia: 1027–1035

Saha S, Moorthi S, Pan HL, Wu XR, Wang JD, Nadiga S, Tripp P, Kistler R, Woollen J, Behringer D, Liu HX, Stokes D, Grumbine R, Gayno G, Wang J, Hou YT, Chuang HY, Juang HMH, Sela J, Iredell M, Treadon R, Kleist D, Van Delst P, Keyser D, Derber J, Ek M, Meng J, Wei HL, Yang RQ, Lord S, Van den Dool H, Kumar A, Wang WQ, Long C, Chelliah M, Xue Y, Huang BY, Schemm JK, Ebisuzaki W, Lin R, Xie PP, Chen MY, Zhou ST, Higgins W, Zou CZ, Liu QH, Chen Y, Han Y, Cucurull L, Reynolds RW, Rutledge G, Goldberg M (2010) The Ncep Climate Forecast System Reanalysis. Bull Am Meteorol Soc 91(8):1015–1057

Thinsungnoen T, Kaoungku N, Durongdumronchai P, Kerdprasop K, Kerdprasop N (2015) The Clustering Validity with Silhouette and Sum of Squared Errors. In: The Proceedings of the 2nd International Conference on Industrial Application Engineering 2015: 44–51

Wang WG, Li HY, Wang J, Hao XH(2020) Water Vapor from Western Eurasia Promotes Precipitation during the Snow Season in Northern Xinjiang, a Typical Arid Region in Central Asia. Water12(1)

Zhao W, Chen W, Chen SF, Yao SL, Nath D(2019) Inter-annual variations of precipitation over the monsoon transitional zone in China during August-September: Role of sea surface temperature anomalies over the tropical Pacific and North Atlantic. Atmos Sci Lett 20(1)